

Dust: Messing with your measurements

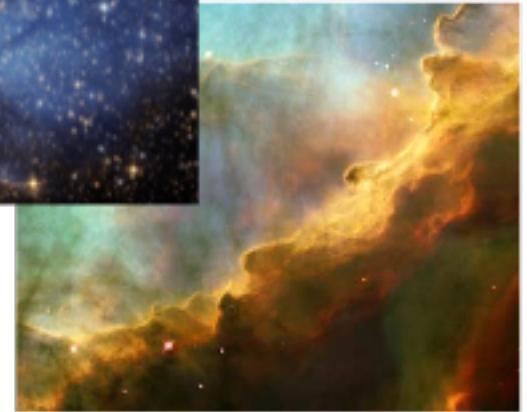


Source: NASA, Hubble

Dust: Prominent in star-forming regions



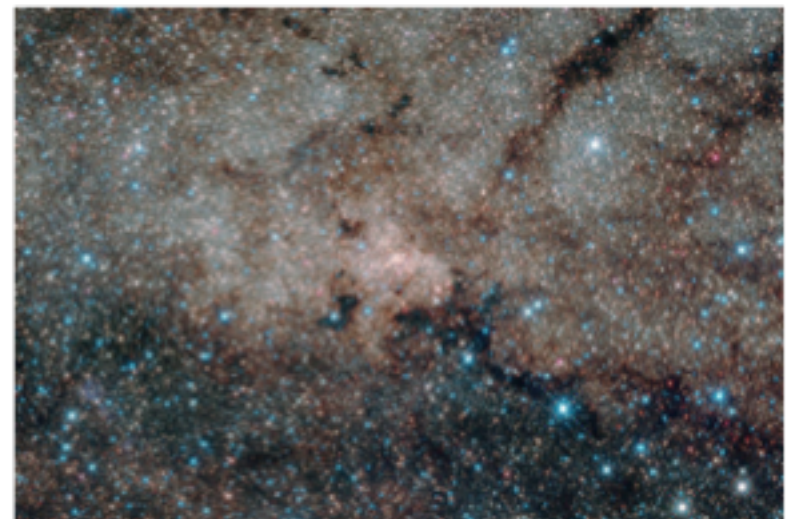
Associated w/
molecular gas



Dust-SF association can be seen globally

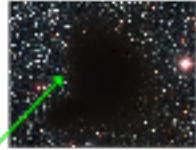


Milky Way dust also obscures distant measurements





Dust plays many important roles in galaxies



- Extinction/Attenuation
- Reddening
- Reprocessing UV/optical light into the infrared
- Scatters light.
- Locks up metals
- Catalyzes formation of H_2

5

Dust

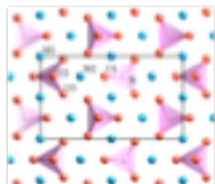
- Extinction, Reddening & Reddening Laws
 - Foreground and Internal Extinction
- Correcting for the Effects of Dust
 - Inclination corrections
 - Balmer Decrements
 - UV slopes
 - Difficulties in deriving A_V .
- Estimating the Amount of Extinction
 - Inclination corrections
 - Balmer Decrements
 - UV slopes
 - Difficulties in deriving A_V .
- Global trends in extinction
- Dust extinction as a tracer of dense gas

6

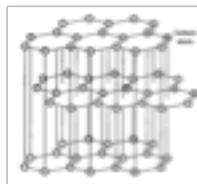
What is dust?

A complex and variable mixture of:

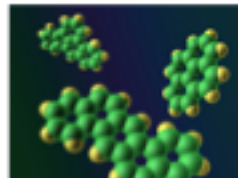
- Large grains ($\sim 0.1\mu m$), made of silicates (SiO complexes bonded with Fe or Mg) and graphite.
- "Coal" (200-2000Å in size)
- "PAH"s: Poly Aromatic Hydrocarbons (like benzene rings)
- "Very small grains" (VSG)



Silicates



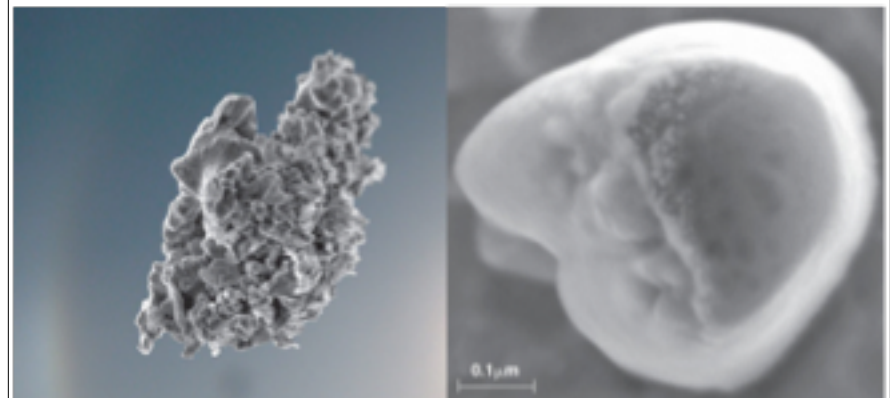
Graphite
Amorphous Carbon



PAHs

7

Cosmic Dust



J. Freitag and S. Messenger

8

The dust population evolves

Dust grains are probably created in:

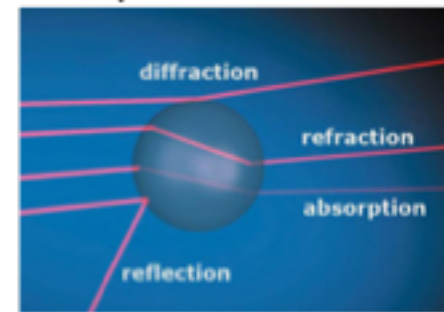
- SN explosions
- Stellar winds (AGB stars in particular)

Dust grains are probably destroyed by:

- Shocks (SN explosions & fast stellar winds)
- Intense radiation

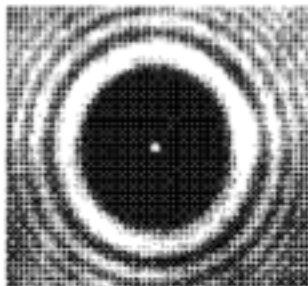
"Dust" refers to a complex population of different grains, with different sizes, that will likely change with environment

Dust has complex interactions with light

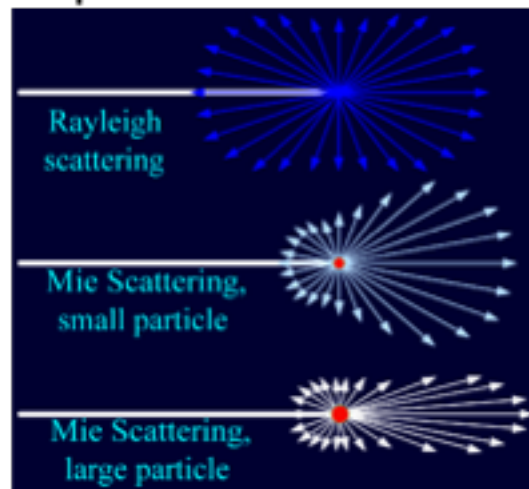


- Interaction depends on size, shape of dust grain
- Affected by composition: affects dielectric constant which then sets complex index of refraction
- Effects calculated as "Mie Scattering": interaction of EM plane wave with $m=n+ik$ index of refraction

Examples of possible effects



Diffraction



Depends on wavelength vs grain size a

$$x = 2\pi a / \lambda$$

Note: Extinction \neq Absorption

Extinction coefficient defined as ratio of cross section for absorption divided by area of spherical grain

$$Q_{\text{ext}} = Q_{\text{abs}} + Q_{\text{scat}}$$

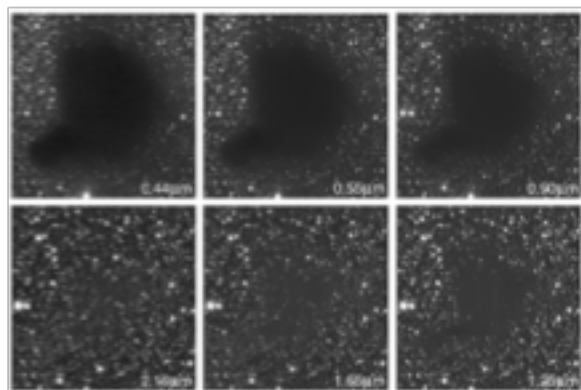
This can be greater than 1, because of scattering

Quantifying dust extinction: Excellent discussion in Binney & Merrifield 3.7

The attenuation in a bandpass X is defined:

$$A_X = (m_{\text{observed}} - m_{\text{true}})_X$$

A_V is usually quoted, for historical reasons

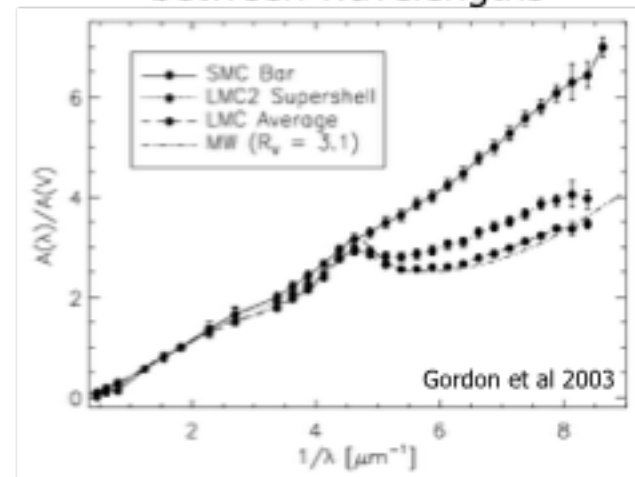


Depends strongly on wavelength.

13

"Attenuation Law"

Describes the relative attenuation between wavelengths

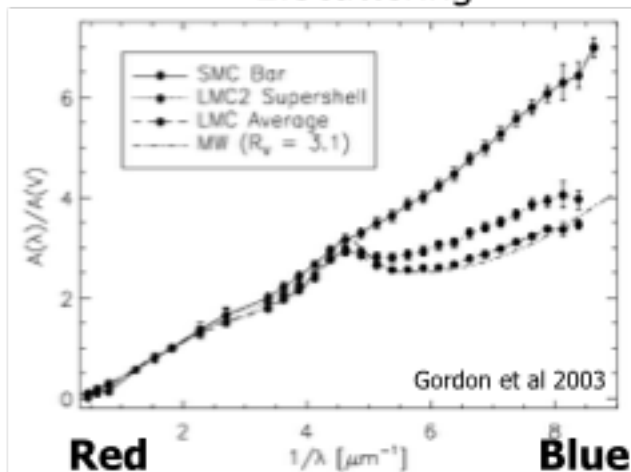


Gordon et al 2003

14 Why inverse wavelength in plot? I have no idea. Someone did it once a long time ago, and now it's the standard...

"Attenuation Law"

2 Contributions: 1. Extinction (i.e. absorption)
2. Scattering

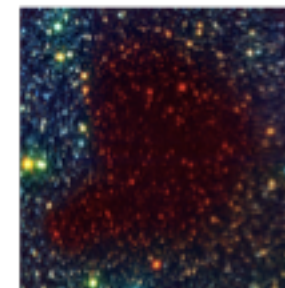


Gordon et al 2003

15 Why inverse wavelength in plot? I have no idea. Someone did it once a long time ago, and now it's the standard...

Reddening

Color-dependent attenuation leads to "reddening"



Definition of reddening (or "color excess")

$$\begin{aligned} E(X-Y) &= (m_X - m_Y)_{\text{observed}} - (m_X - m_Y)_{\text{true}} \\ &= (m_{\text{observed}} - m_{\text{true}})_X - (m_{\text{observed}} - m_{\text{true}})_Y \\ &= A_X - A_Y \end{aligned}$$

$E(B-V)$ is usually quoted, for historical reasons

16

Attenuation curves sometimes plotted in terms of reddening

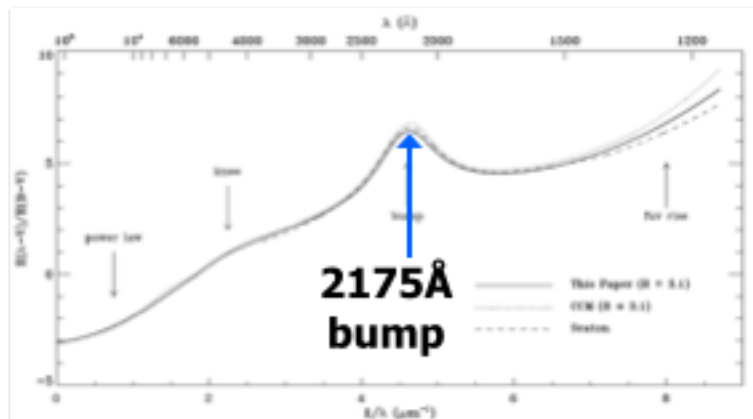
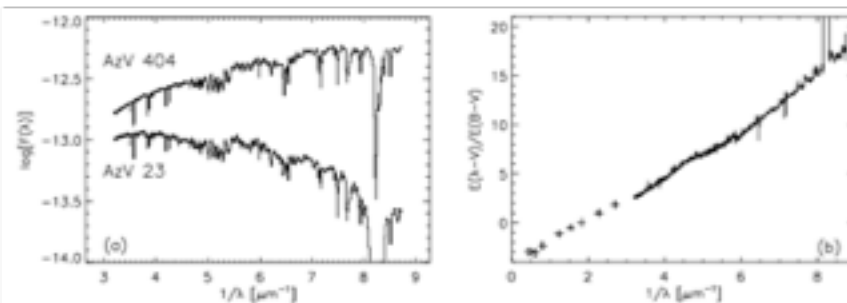


FIG. 1 — Standardized interstellar extinction curves from the far-IR through the UV. Several general features of the curves are noted. The solid and dotted curves are estimates for the case $R = A(V)/E(B-V) = 3.1$ derived in the Appendix of this paper and by Cardelli, Clayton, & Mathis 1989, respectively. The dashed curve shows the average Galactic UV extinction curve from Seaton (2005).

Fitzpatrick et al 1999

Measuring the Attenuation Law



Use pairs of stars with identical spectral types (i.e. absorption features)

Gordon et al 2003

Optical attenuation in different bandpasses

Filter	λ_{eff} (Å)	$A(\lambda)/A(V)$	$A(\lambda)/E(B-V)$	Filter	λ_{eff} (Å)	$A(\lambda)/A(V)$	$A(\lambda)/E(B-V)$
Landolt U	3372	1.664	5.434	Strömgren u	3900	1.602	5.231
Landolt B	4404	1.321	4.315	Strömgren b	4676	1.240	4.049
Landolt V	5428	1.015	3.315	Strömgren v	4127	1.394	4.552
Landolt R	6509	0.819	2.671	Strömgren β	4961	1.182	3.858
Landolt I	8090	0.594	1.940	Strömgren γ	5479	1.094	3.277
CTIO U	3683	1.518	4.968	Sloan u'	3546	1.579	5.155
CTIO B	4393	1.324	4.325	Sloan g'	4925	1.161	3.793
CTIO V	5519	0.992	3.240	Sloan r'	6315	0.845	2.771
CTIO R	6602	0.807	2.634	Sloan i'	7799	0.679	2.086
CTIO I	8046	0.601	1.962	Sloan z'	9294	0.453	1.479
UKIRT J	12660	0.276	0.902	WFPC2 F300W	3047	1.791	5.849
UKIRT H	16732	0.176	0.576	WFPC2 F450W	4711	1.229	4.015
UKIRT K	22152	0.112	0.367	WFPC2 F555W	5498	0.996	3.252
UKIRT L	38079	0.047	0.153	WFPC2 F606W	6042	0.885	2.889
Gunn g	5244	1.065	3.476	WFPC2 F702W	7068	0.746	2.435
Gunn r	6707	0.793	2.590	WFPC2 F814W	8066	0.597	1.948
Gunn i	7985	0.610	1.991	DESS-II g	4114	1.197	3.907
Gunn z	9055	0.472	1.540	DESS-II r	6371	0.811	2.649
Spiral R_s	6993	0.755	2.467	DESS-II i	8183	0.580	1.893
APM R_p	4690	1.236	4.093				

NOTE.—Magnitudes of extinction evaluated in different passbands using the $R_v = 3.1$ extinction laws of Cardelli et al. 1989 and O'Donnell 1994. The final column normalizes the extinction to photometric measurements of $E(B-V)$.

Note: Corrections given in Schlafly & Finkbeiner 2011

Schlegel et al 1998

Attenuation in the IR

λ	$E(B-V)/E(B-V)$	A_λ/A_V	van de Hulst No. 15
U	1.64 ^a	1.531	1.555
B	1.00 ^a	1.324	1.329
V	0.0 ^a	1.000	1.000
R	-0.78 ^a	0.748	0.738
I	-1.60 ^a	0.482	0.469
J	-2.22 ± 0.02	0.282	0.246
H	-2.55 ± 0.03	0.175	0.155
K	-2.744 ± 0.024	0.112	0.0885
L	-2.91 ± 0.03	0.058	0.045
M	-3.02 ± 0.03	0.023	0.033
N	-2.93	0.052	0.013
8.0 μ m	-3.03	0.020 ± 0.003	
8.5	-2.96	0.043 ± 0.006	
9.0	-2.87	0.074 ± 0.011	
9.5	-2.83	0.087 ± 0.013	
10.0	-2.86	0.083 ± 0.012	
10.5	-2.87	0.074 ± 0.011	
11.0	-2.91	0.060 ± 0.009	
11.5	-2.95	0.047 ± 0.007	
12.0	-2.98	0.037 ± 0.006	
12.5	-3.00	0.030 ± 0.005	
13.0	-3.01	0.027 ± 0.004	

^a From Nandy et al. 1976.

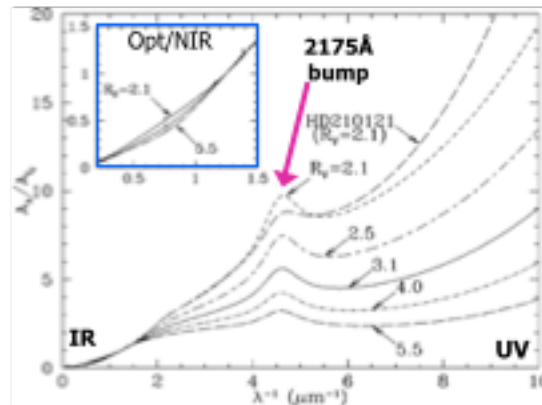
^b From Schultz and Wiener 1975.

Rieke & Lebofsky 1985

Attenuation laws characterized by R_V

$$R_V = A_V / (A_B - A_V) = A_V / E(B-V)$$

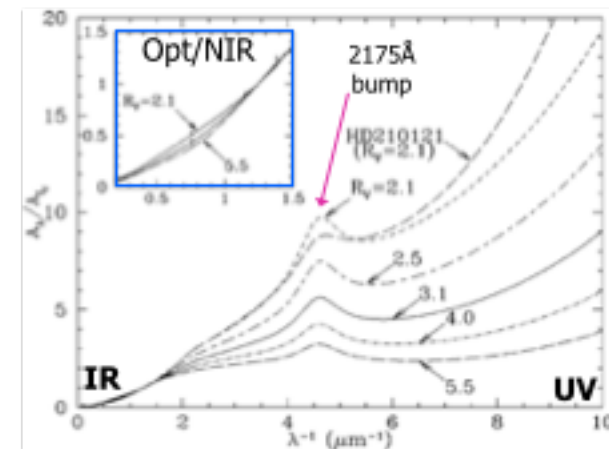
Related to the slope of the extinction curve near the V band



Smaller R_V =
More wavelength
dependence,
more reddening
for a given
extinction A_V

21

Attenuation Law Functional Forms

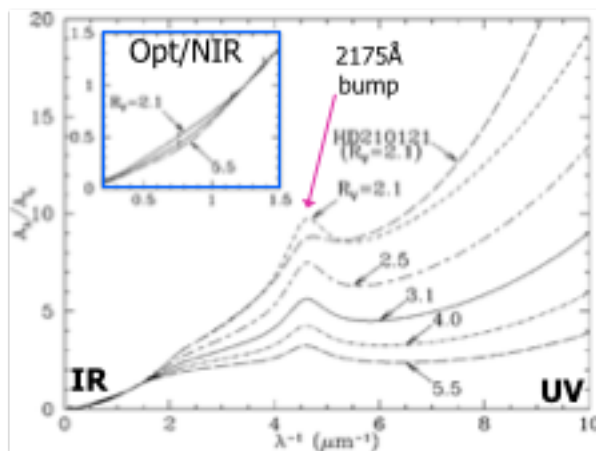


Draine 2003
ARA&A

Family of curves $A_\lambda / A_V \approx f(\lambda; R_V, C_1, C_2, C_3, C_4, \lambda_0, \gamma)$
defined by different
values of R_V
Cardelli, Clayton, & Mathis (CCM) 1989
Fitzpatrick 1999

22

Attenuation Law Functional Forms



FUV
curvature
(fixed)

Family of curves $A_\lambda / A_V \approx f(\lambda; R_V, C_1, C_2, C_3, C_4, \lambda_0, \gamma)$
defined by different
values of R_V
Depends largely on R_V
2175Å bump
(fixed)

23

Wide variation, but $R_V=3.1$ is "typical"

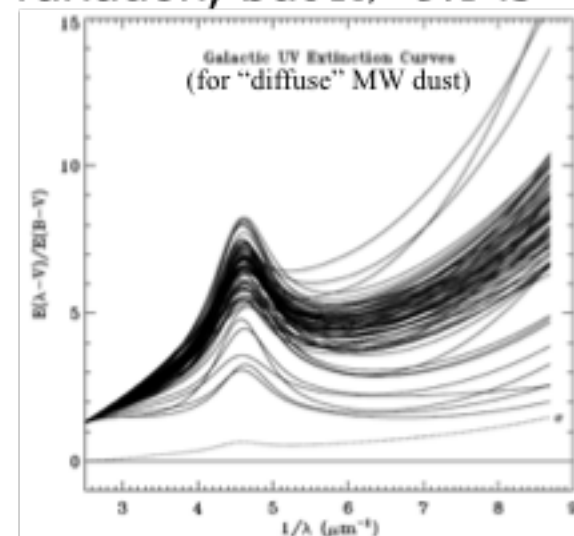


FIG. 2. — Examples of MW-Galactic UV extinction curves derived from IUE satellite observations. Analytical fits to the curves are shown, based on the work of Fitzpatrick & Staszko (1998). The curves are taken from the Fitzpatrick & Staszko catalog, with the addition of the lines of sight toward HD 150121 from Whitty & Fowler (1991) and HD 150121-1 from Cardelli & Savage (1995). This figure demonstrates the enormous range of properties exhibited by UV extinctions in the Milky Way. The dotted line, labeled "1", shows the standard deviation of the sample scaled to the value $\sigma(1.900) = 0.14$, as derived from IUE satellite data (see §3.2).

24

Fitzpatrick et al 1999

Lines of sight with more dust-per-gas tend to have larger R_V

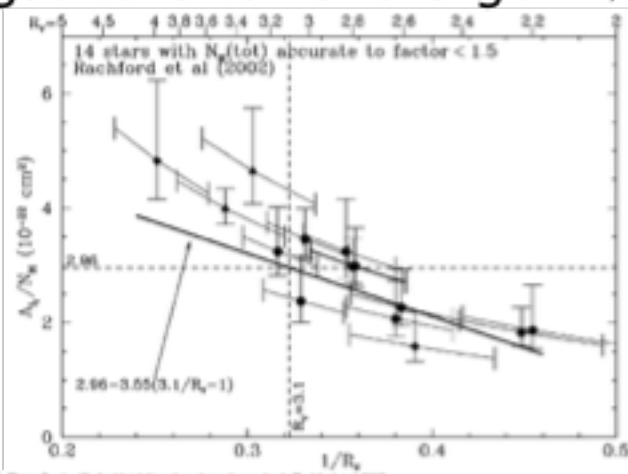


Figure 3. A_V/N_H for 14 sightlines through translucent clouds (Rachford et al. 2002), as a function of $1/R_V$, with R_V determined by 10 photometry studies. $R_V = 3.1 \pm 0.2$ (photometry N_H triangles, $R_V = 3.1 \pm 0.2$ or 10% extinction curve (diamonds, $R_V = 3.1 \pm 0.2$). Vertical error bars show 1- σ uncertainty due to errors in N_H ; solid error bars show effects of errors in R_V . Least-squares fit (Equation 5) is shown.

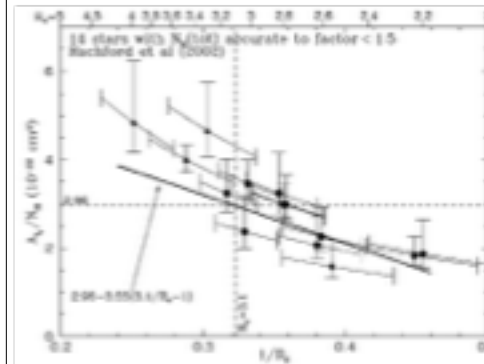
Draine 2003

Expectations for R_V :

Large Grains
("grey extinction")
 $R_V = \infty$

Raleigh Scattering:
 $R_V \approx 1.2$

Dustier clouds have proportionally more large grains



25

Different types & sizes of grains produce different features

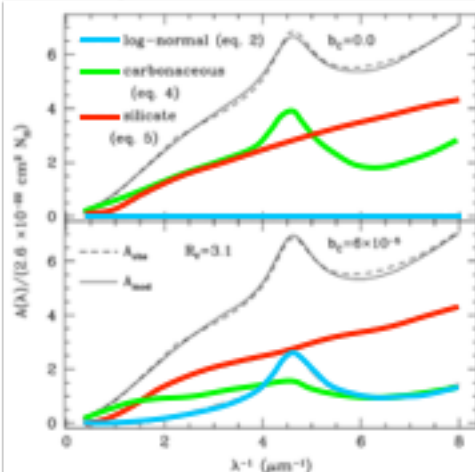
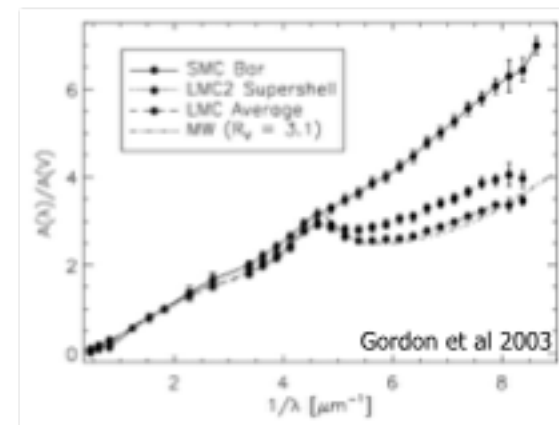


FIG. 8.—Extinction curve A_{tot} resulting from the grain distribution of eqs. (4) and (5), with parameters optimized to fit A_{tot} (see text) for $R_V = 3.1$ (also shown), for $b_V = 0.0$ and 6.0×10^{-4} . The contributions from the three grain distribution components are also shown.

silicates
PAHs + carbonaceous
very small grains
silicates
very small grains
PAHs + carbonaceous

Weingartner & Draine 2001

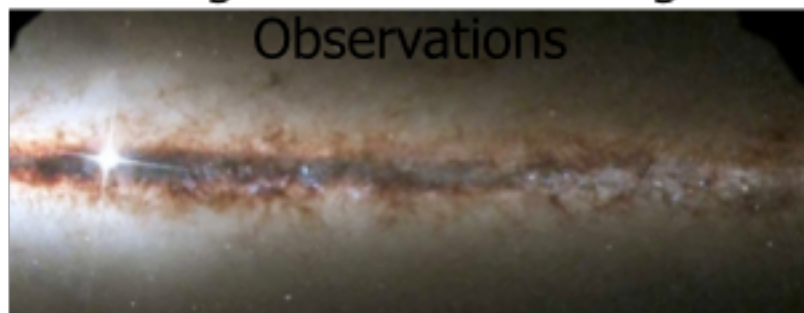
Different galaxies have different mean extinction curves



Different average dust composition

26

Correcting for Dust in Extragalactic Observations



- Foreground Extinction
 - removing effects of the Milky Way
- Internal Extinction
 - removing effects of dust within the observed galaxy

29

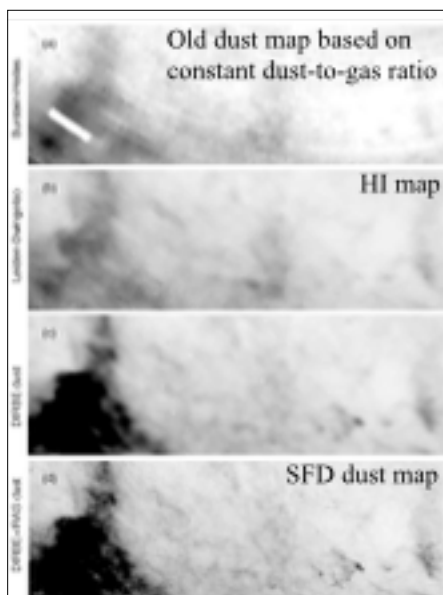
Within the Milky Way, dust extinction can be constrained by combinations of star counts and colors



Important because:

- Light that we observe from extragalactic objects pass through the MW's dust.
- Extinction is a good tracer of molecular gas

30



Milky Way Dust:
Schlegel, Finkbeiner,
& Davis 1998 (SFD)

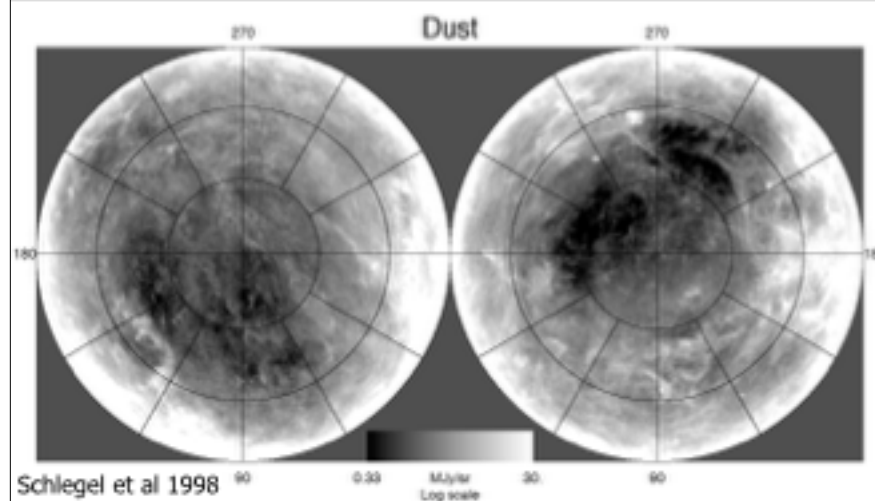
“Foreground Extinction”

- Use black body FIR emission from dust to determine the temperature of dust.
- Combine with maps of FIR emission to measure column density of dust.

Schlegel et al 1998

FIG. 7.—Slice of sky from (a) the HI map, (b) the Leiden-Deinze H I map, (c) our dust map with DEDIE resolution, and (d) our dust map with DEDIE resolution. The slice measures approximately $30^\circ \times 30^\circ$, centered at $l = 100^\circ$, $b = +33^\circ$.

Not uniform! No “dust free” sitelines

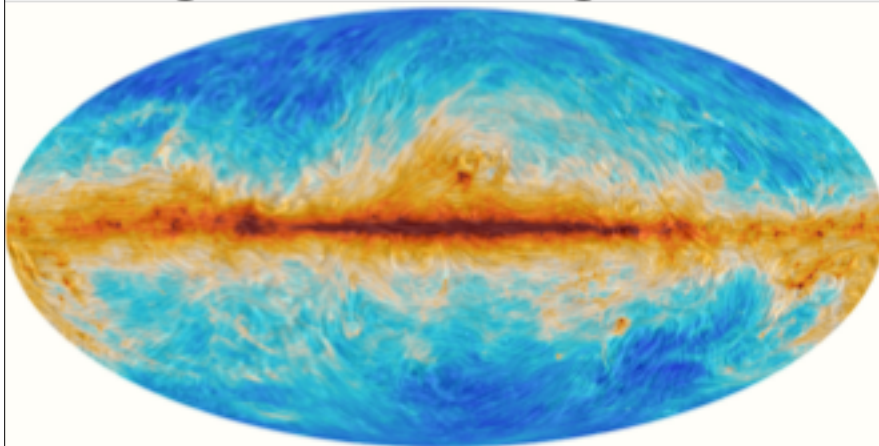


Schlegel et al 1998

All extragalactic observations must correct for this!

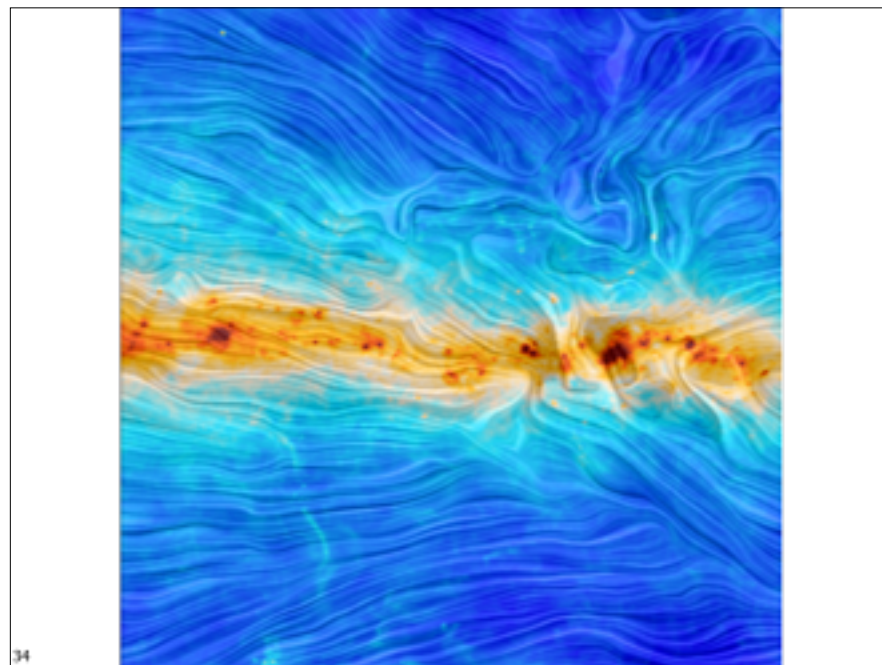
32 Note: See Schlafly & Finkbeiner 2011 for PS-1 recalibrated maps

MW dust emission is polarized, due to alignment with magnetic field



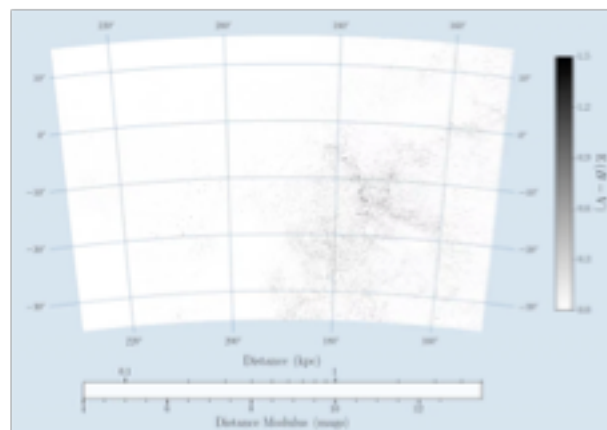
Results from Planck Collaboration 2015

³³ Nice visualizations: <http://astrog80.astro.cf.ac.uk/Planck/Chromosome/>



New 3-D Milky Way dust maps out to
~5 kpc from Pan-STARRS available

Green et al 2014,2015



Galactic Anti-center

<http://argonaut.skymaps.info>

Warning: Extinction law of high-latitude dust is unusual

Optical
galaxy color
vs SFD
extinction:
 $R_V=3.1$

UV galaxy
color vs SFD
extinction:
 $R_V=2.2$

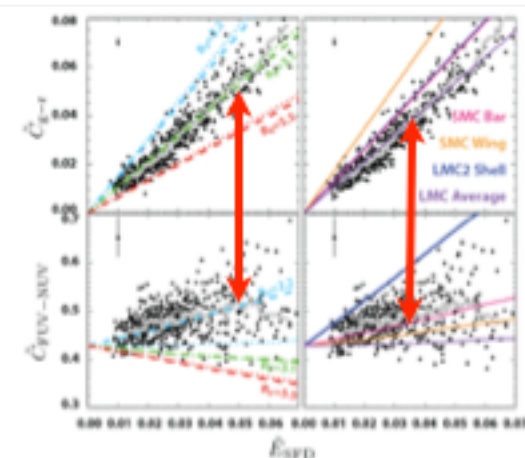
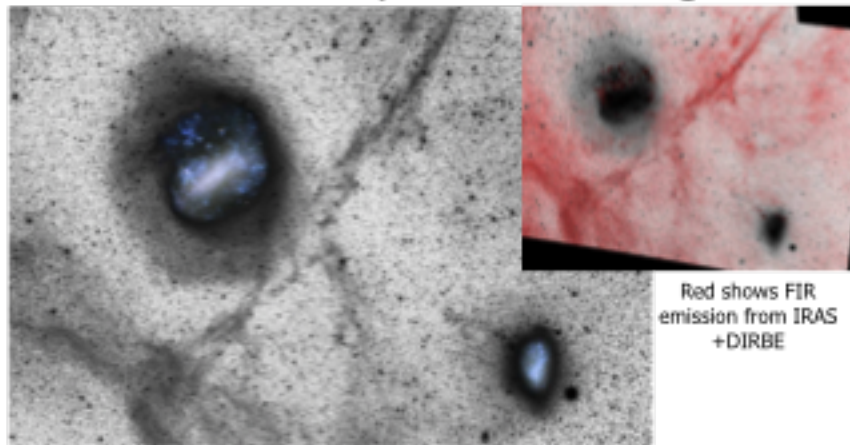


Figure 8. *Large system galaxy rates.* \bar{C} . Top left panel shows data from the GALEX-WISE galaxy sample, bottom left shows data from SDSS-PS2 galaxy sample, both matched to the WISE footprint, for comparison. The gray lines show the surface galaxy rate as a function of flux. Also shown are GALEX infrared and PS2 infrared, combining counts with $S/N \geq 1.5$, and 1.5 σ limits, green, and red, respectively. Right, subtracting low S/N counts of separating the color variation in both the optical and IR. On the right the same data as shown with four magnitude bins (dashed lines) from Fardas et al. (2006). Note that for these selection criteria each data

Peck & Schminovich 2013

Warning: the dusty high-latitude "cirrus" emits at red optical wavelengths



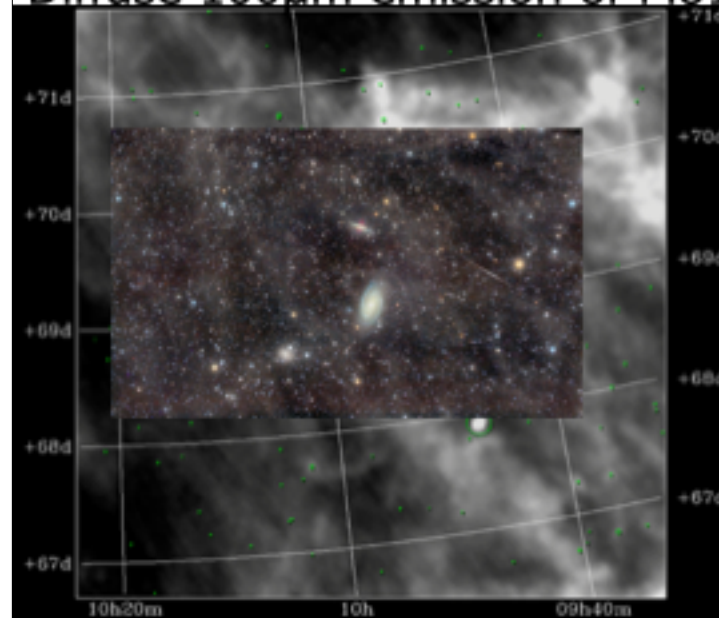
Red shows FIR emission from IRAS + DIRBE

- Probably due to photoluminescence of dust.
- Sometimes referred to as ERE "extended red emission"

see early work by Guhathakurta & Tyson 1990, Szomoru & Guhathakurta 1998

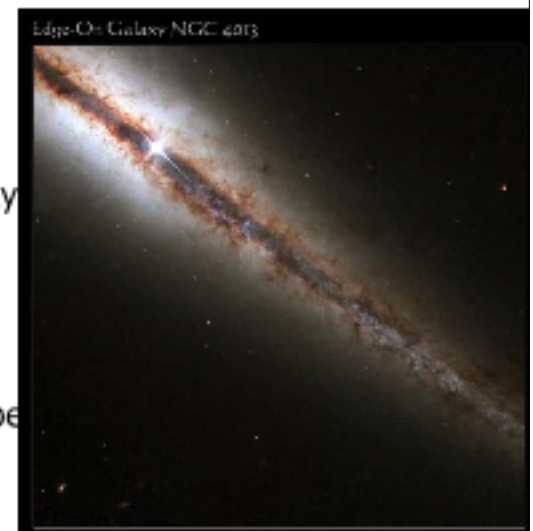
37

Diffuse 100 μ m emission of M81 group



"Internal Extinction Corrections":
account for galaxies' own dust

- Brings all galaxy magnitudes to those expected if the galaxy were seen face-on.
- Depends on inclination, wavelength, and galaxy luminosity/type



Dominant limitation on faint surface photometry

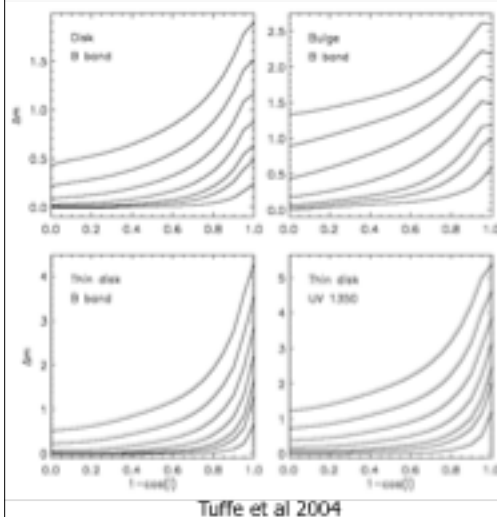


<http://apod.nasa.gov/apod/ap120313.html>

39

40

Internal extinction vs inclination



Model of normal spirals with different total face-on optical depths

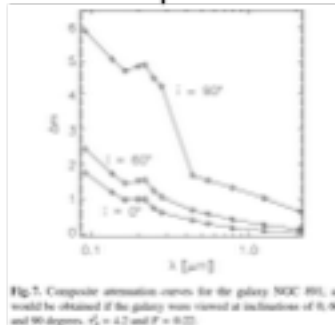
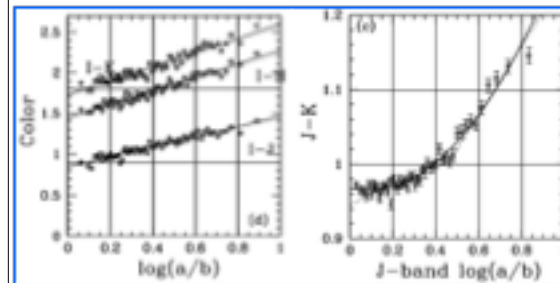


Fig. 5. Composite attenuation curves for the galaxy NGC 491, as would be obtained if the galaxy was viewed at inclinations of 0, 90 and 90 degrees. $r_d = 4.7$ and $r_b = 0.25$.

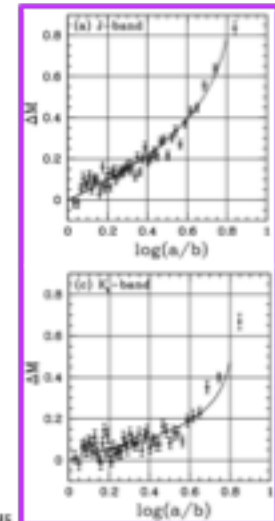
Fig. 2. Examples of the dependence of attenuation (A_v) on inclination (i) for the main geometrical components of our model: disk (top left), bulge (top right), and thin disk (bottom left and right). The examples are plotted for the B band for the disk and bulge, and both for the B band and UV 1350 Å for the thin disk. In each panel we plotted (from top to bottom) 7 attenuation curves, corresponding to r_d : 8, 4, 2, 1, 0.5, 0.3, and 0.1. The face-on orientation corresponds to $1 - \cos i = 0.0$ and the edge-on orientation corresponds to $1 - \cos i = 1.0$.

Internal Extinction: Estimate from inclination, using empirical color dependence



Masters et al 2003

Use the observed color/magnitude offset as a function of inclination to derive the necessary inclination correction



42 See also Tully et al 1998, Matthews et al 1998, Piemi 1999, Boselli.

Internal extinction: Estimate correction from "Balmer Decrement"

The value of the Balmer extinction is derived from the observed ratio of $H\alpha$ and $H\beta$ line intensities using the relation

$$C(H\beta) = \frac{1}{f(H\beta) - f(H\alpha)} \log \frac{I(H\alpha)/I(H\beta)}{I^0(H\alpha)/I^0(H\beta)} \quad (1)$$

where $I^0(H\alpha)/I^0(H\beta)$ is the intrinsic intensity ratio of these two lines and $f(H\beta) - f(H\alpha)$ is equal to 0.335. The value

- In "case B" recombination, $H\alpha$ and $H\beta$ are always emitted in the same ratio.
- $H\beta$ is emitted at a **shorter** wavelength, and will thus suffer more extinction than $H\alpha$.
- The observed ratio of $H\alpha/H\beta$ **increases** with extinction

Internal extinction: Estimate correction from the slope of the UV spectrum

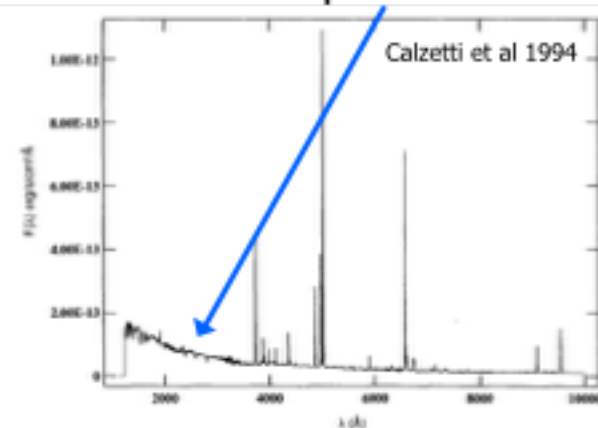


Fig. 2.—An example of UV and optical spectrum with no normalization between the two wavelength ranges. The galaxy is NGC 5253. The flux in $\text{ergs cm}^{-2} \text{s}^{-1} \text{\AA}^{-1}$ is plotted as a function of the wavelength λ in the range 1220–10000 Å. The joining point between the UV and optical is at 3200 Å.

Most star bursts have a reasonably constant power-law slope at UV wavelengths (tail of O/B star blackbody).

If redder, then probably due to dust

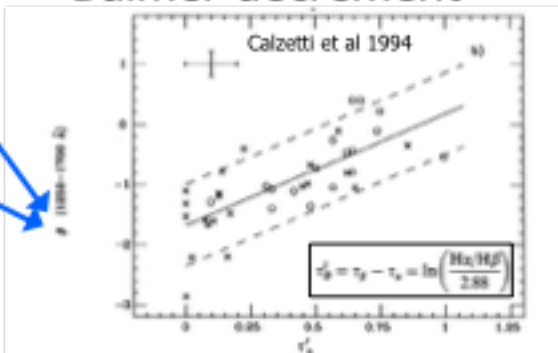
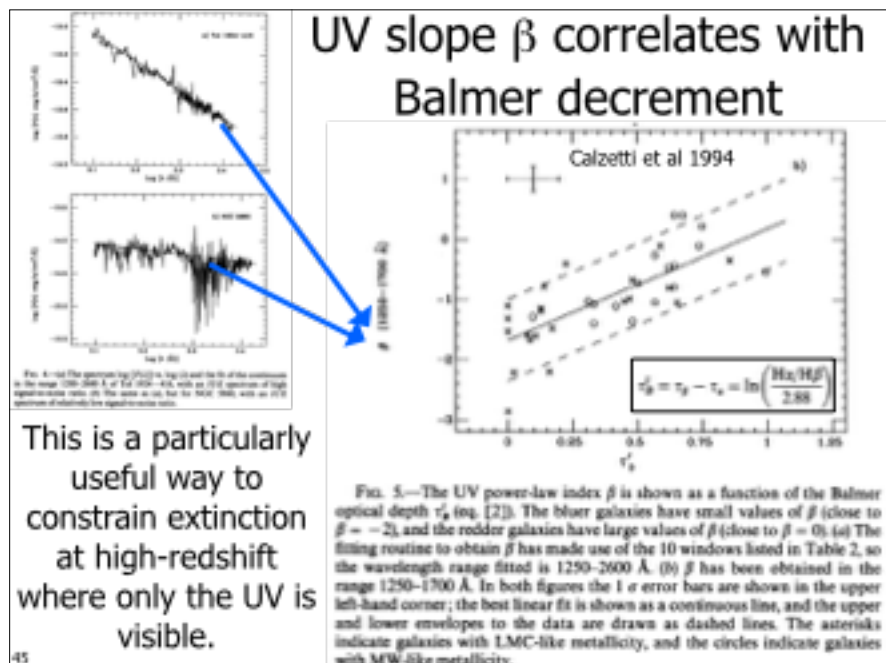


FIG. 5.—The UV power-law index β is shown as a function of the Balmer optical depth τ_B (eq. [2]). The bluer galaxies have small values of β (close to $\beta = -2$), and the redder galaxies have large values of β (close to $\beta = 0$). (a) The fitting routine to obtain β has made use of the 10 windows listed in Table 2, so the wavelength range fitted is 1250–2600 Å. (b) β has been obtained in the range 1250–1700 Å. In both figures the 1σ error bars are shown in the upper left-hand corner; the best linear fit is shown as a continuous line, and the upper and lower envelopes to the data are drawn as dashed lines. The asterisks indicate galaxies with LMC-like metallicity, and the circles indicate galaxies with MW-like metallicity.

Templates that fit the empirical correlation:

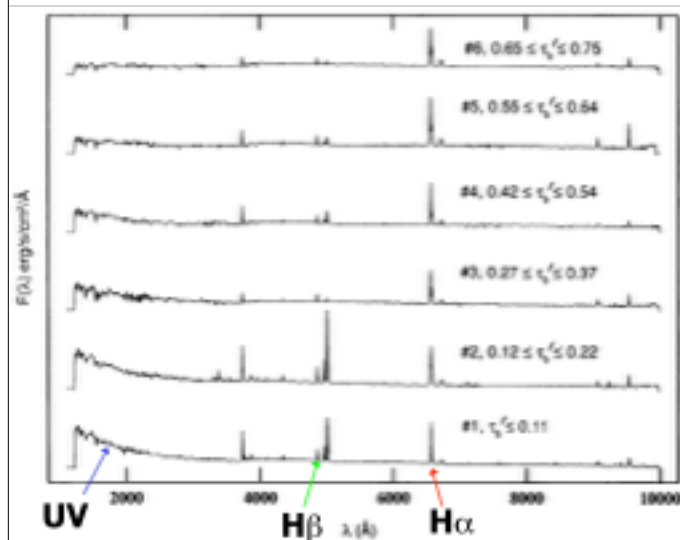


FIG. 17.—The spectra of the six templates are shown for increasing values of the extinction parameter τ_B , from the bottom to the top of the figure.

Reddening (observed Balmer decrement &/or UV slope) \neq Total extinction

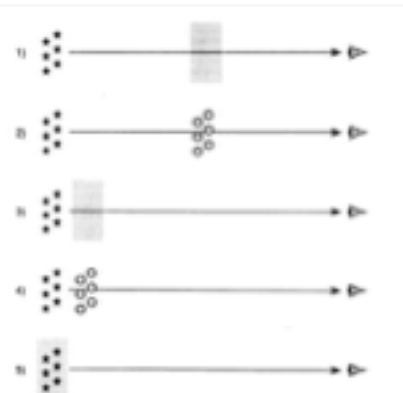
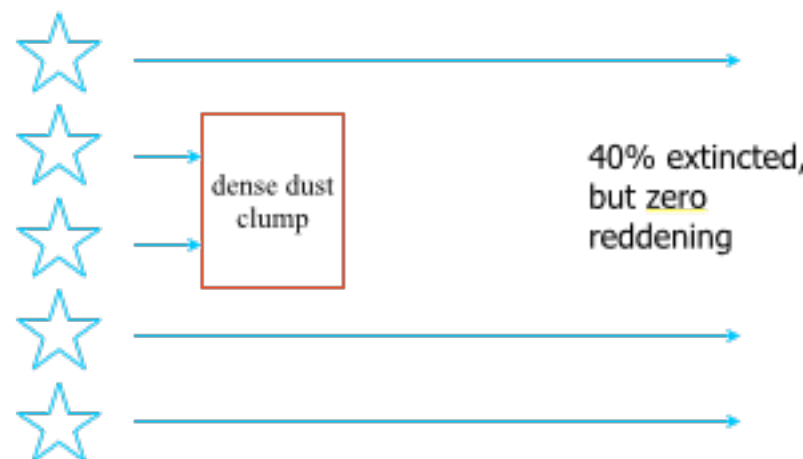


FIG. 3.—A schematic representation of the five configurations of dust/ionized gas discussed in § 4. From top to bottom, they are (1) the uniform dust screen, (2) the clumpy dust screen, (3) the uniform scattering slab, (4) the clumpy scattering slab, (5) the internal dust model.

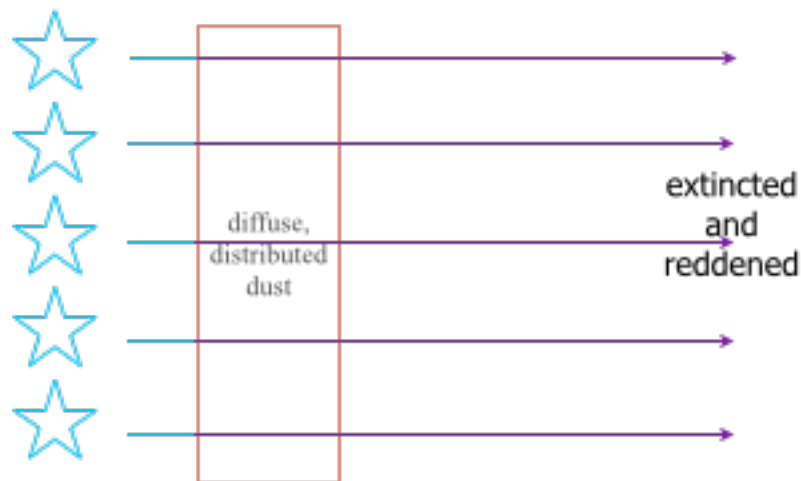
Problem 1: Can produce arbitrary combinations of reddening and extinction by varying the relative distributions and clumpiness of the dust and the stars

Calzetti et al 1994

Why dust geometry decouples reddening and extinction:



Why dust geometry decouples reddening and extinction:



49

Reddening (observed Balmer decrement & UV slope) \neq Total extinction

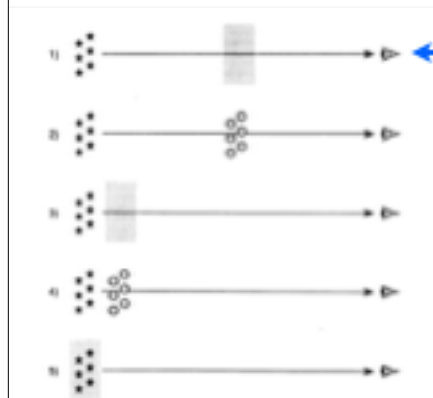


FIG. 3.—A schematic representation of the five configurations of dust/ionized gas discussed in § 4. From top to bottom, they are (1) the uniform dust screen; (2) the clumpy dust screen; (3) the uniform scattering slab; (4) the clumpy scattering slab; (5) the internal dust model.

Everything reddened,
everything extincted,
little scattering

Calzetti et al 1994

50

Reddening (observed Balmer decrement & UV slope) \neq Total extinction

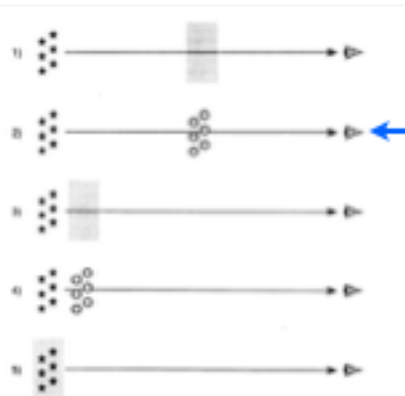


FIG. 3.—A schematic representation of the five configurations of dust/ionized gas discussed in § 4. From top to bottom, they are (1) the uniform dust screen; (2) the clumpy dust screen; (3) the uniform scattering slab; (4) the clumpy scattering slab; (5) the internal dust model.

Some stars reddened
and more heavily
extincted, other stars
unobscured, little
scattering

Calzetti et al 1994

51

Reddening (observed Balmer decrement & UV slope) \neq Total extinction

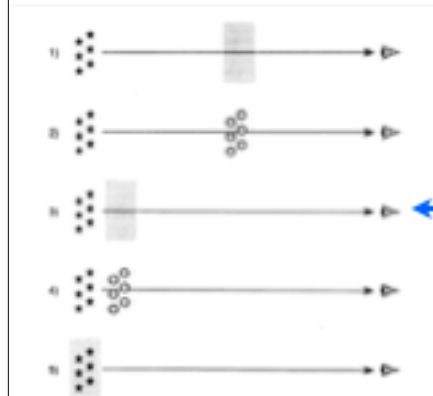


FIG. 3.—A schematic representation of the five configurations of dust/ionized gas discussed in § 4. From top to bottom, they are (1) the uniform dust screen; (2) the clumpy dust screen; (3) the uniform scattering slab; (4) the clumpy scattering slab; (5) the internal dust model.

Everything reddened,
everything extincted,
lots of scattering

Calzetti et al 1994

52

Reddening (observed Balmer decrement & UV slope) \neq Total extinction

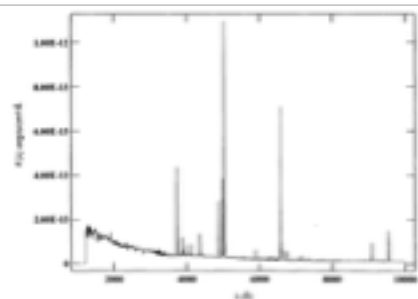


Fig. 2.—An example of UV and optical spectrum with no normalization between the two wavelength ranges. The galaxy is NGC 5255. The flux is $\text{ergs cm}^{-2} \text{s}^{-1} \text{\AA}^{-1}$ is plotted as a function of the wavelength λ in the range 1220–10000 Å. The joining point between the UV and optical is at 3200 Å.

Problem 2: The extinction and/or reddening in different parts of the spectrum may be caused by different dust structures

Dust in HII regions \neq Dust near exposed O/B stars \neq Dust in field stars that dominate the red continuum

Reddening (observed Balmer decrement & UV slope) \neq Total extinction

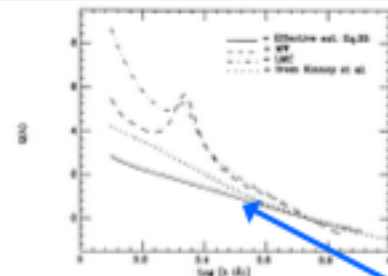


Fig. 21.—The extinction law derived in this work (eq. (20), continuous line) is compared with the Milky Way (dashed line) and the LMC (dash-dotted line) extinction laws. The extinction law derived by Kinney et al. (1996b) is also shown (dotted line). The zero point of the four curves is arbitrary and has been chosen to be the value $A(5500) = 0.6$.

Problem 3: The extinction law may vary from galaxy to galaxy, or within different parts of the same spectrum, due to variations in dust content

Extinction law for HII regions & UV in starbursts seems "greyer" than typical MW extinction

Global Trends in Dust Extinction

- Galaxy-to-Galaxy
- Within Galaxies

Lower mass, late-type disks have less extinction.

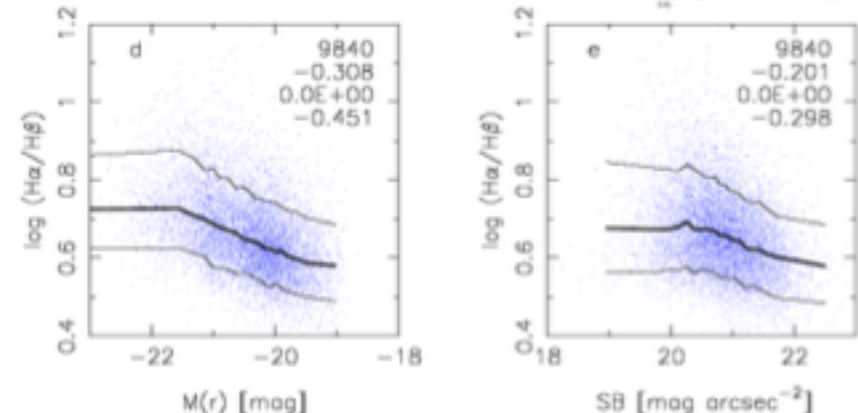
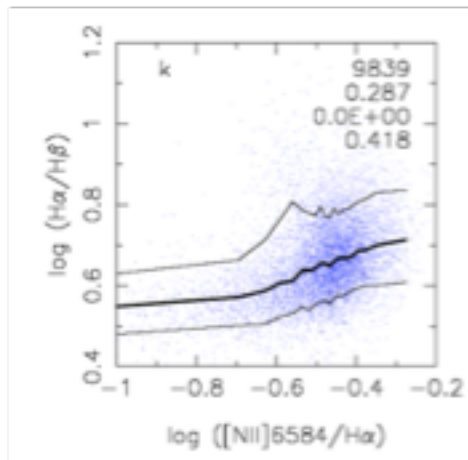
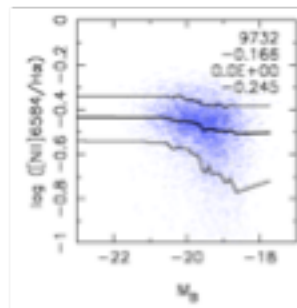
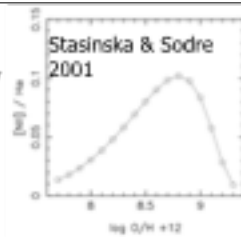


Fig. 6. The relation between $\log(H\alpha/H\beta)$ and various properties of the galaxy. The meaning of the numbers in the upper right is the same as in Fig. 5. The thick curve represents the median value of $\log(H\alpha/H\beta)$. The thin curves define the zone containing 80% of the data points (see Sect. 3.1).

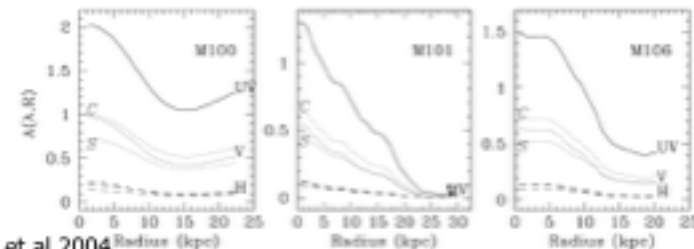
This trend is probably partially (but not completely) driven by metallicity



[NII]/H α is a reasonable metallicity indicator, and low luminosity galaxies have low metallicity, & thus less dust



Within spiral disks, extinction drops with radius



Bossier et al 2004

Fig. 9. Extinction profiles in the UV, V and R. $A(λ, R)$ is obtained from the FBR/UV ratio. The black line shows the extinction profiles in V and R as derived for a sandwich model with dust-to-star scale-height ratio ℓ depending on the wavelength. For each of these two bands, the others curve show the predicted extinction for a dust screen with Milky-Way-type dust (N) and the Calzetti (1999) law (C).

- Outer regions of disks have similar properties to the inner regions of low mass, low surface density disks.

62

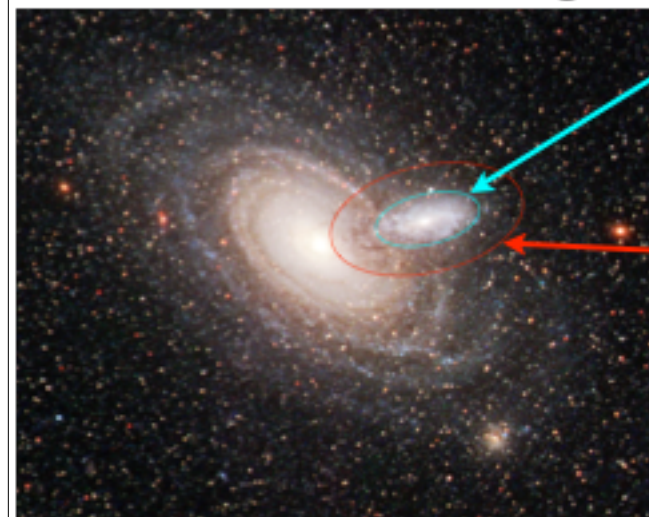
Empirical constraints come from a few cases where galaxies are seen in projection

Spiral Galaxy Pair NGC 3314



Galaxies tend to be opaque in their spiral arms, but optically thin between them.

Dust exists at large radii.



Stars peter out here...

Dust continues out to here.

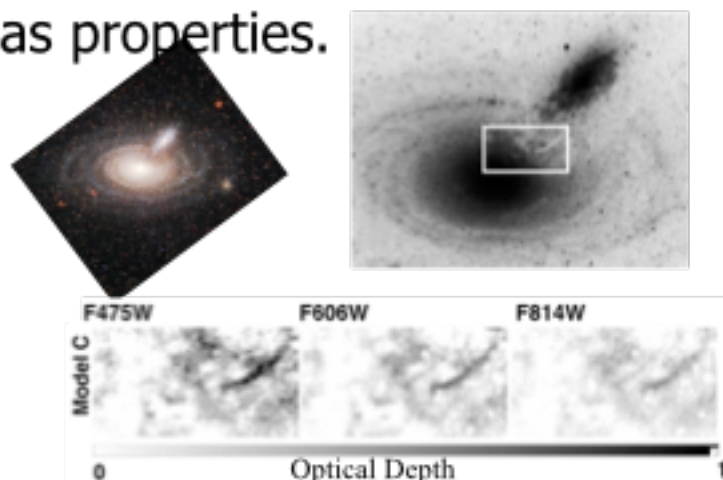
(i.e. there is dense gas at large radii!)

Foreground galaxy silhouette

Holwerda et al 2009

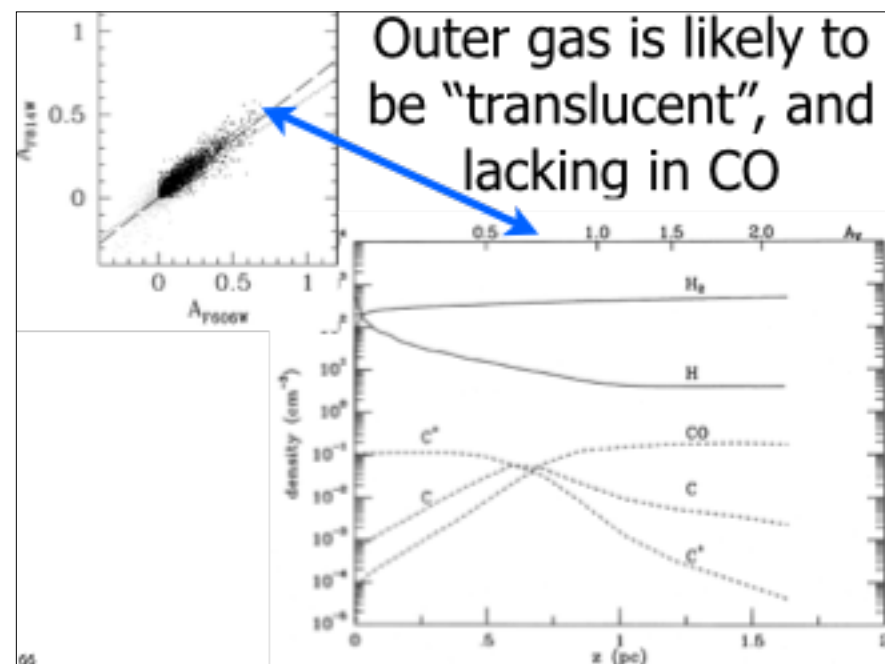
64

Use attenuation maps to constrain gas properties.



No high optical depths with $A_V > 1$

65

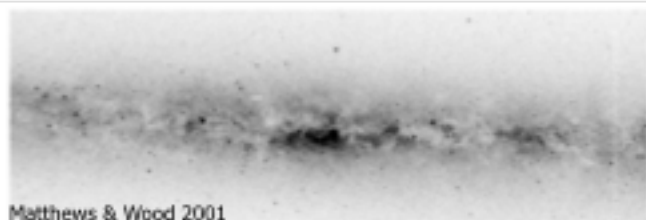


65

Geometry: Dust lanes in massive galaxies



But in low mass galaxies ($V_c < 120 \text{ km/s}$), dust layer is thicker and more diffuse Dalcanton et al 2004



Matthews & Wood 2001

Fig. 1. — $F475W + F606W + F814W$ composite image of a portion of the disk of NGC 1705, as imaged by the Wide Field and Panchromatic Camera (WFPC2) onboard the Hubble Space Telescope. This is an $10'' \times 10''$ portion of the disk, centered near $r = 0$. The resolution is $\sim 0.1''$. The white circle around the position of the galaxy indicates the position of the galaxy.

67

Unusual Dust in Unusual Galaxies



68